Aries Rocket Motor Infrared and Ultraviolet Spent-Stage Emission

D. S. Frankel* and M. E. Gersh†
Aerodyne Research, Inc., Billerica, Massachusetts
and
A. McIntyre,‡ R. E. Huffman,§ and D. E. Paulsen¶
Air Force Geophysics Laboratory, Hanscom AFB, Bedford, Massachusetts

Data from accidental observations of the Aries booster spent-stage emission by the Multispectral Measurements Program TEM-1 flight sensors are presented and analyzed. Large sources of infrared radiation from H_2O, CO, CO_2, and HCl were observed more than 300 s after the nominal booster burnout. Emission in the 7-12 μ region from large polyatomic organic molecules was also observed. Ultraviolet radiation was observed to increase with increasing atomic oxygen density on descent. This uv radiation is probably due to chemiluminescent reactions of combustion fragments with atomic oxygen. These observations should be of value to all who use solid-fueled rockets for launching scientific payloads.

Introduction

SCIENTIFIC sounding rocket payloads are usually carried to their design altitude by solid-fueled rocket motors. Well-designed propellant loadings are constructed to reach burnout at a precise time, with their thrust dropping from 100% to near zero in a time interval on the order of 1 s. This is desirable from the point of view of predicting booster performance and for the operation of the scientific instruments in the payload.

Problems with this simple picture have become more evident as the instruments in the payloads became more sensitive and demanding of their environment. In this paper, we report results of the Multispectral Measurements Program (MSMP) TEM-1 experiment. Unplanned excursions of the TEM-1 sensor module line of sight provided data on infrared and ultraviolet emissions from the "spent" solid-fueled Aries[1] booster. This spent-stage emission was of large spatial extent and could interfere with the intended measurements in these wavelength regions. Indeed, our observations are similar in many ways to "unidentified emissions" already reported by others under similar circumstances in both the infrared[2,3] and ultraviolet[4] spectral regions. It is hoped that our observations will be useful in the design of future experiments using solid rocket boosters.

The Experiment

The TEM-1 payload consisted of a target engine and a sensor module. The target engine, whose plume properties the MSMP experiment was designed to measure, was mounted above the Aries booster. The sensor module, containing the optical instruments, was mounted above the target engine. The nose cone contained the sensor module attitude control and recovery systems.

The planned launch trajectory took the payload to a peak altitude above 220 km, with an impact point on the ground some 60 km north of the launch site. Booster burnout (nominal) occurred at 63 s after ignition, while separation of the payload did not occur until $t=80$ s. The separation velocity was about 1 m/s. From $t=25$ s until separation, the booster was slightly inclined from the vertical (elevation angle 85 deg) with its axis in a north-south plane. After separation, there was no direct indication of booster attitude.

The sensor module was intended to be aimed at the target engine during and between target engine measurement burns. In fact, the sensor attitude control system failed in such a way that the sensor tumbled freely. As a result, the sensor line of sight at various times approached the booster, the airglow layer, and the Earth. Data collected during chance excursions of the line of sight through airglow layers are described and analyzed elsewhere.[5]

The MSMP TEM-1 sensor module included both infrared (i.r.) and uv instruments. A partial listing of these instruments and some of their properties is given in Table 1.

In the infrared, the full-field radiometer (FFR) data are continuous, giving an easily interpreted overview of what happened during the flight. The circular variable filter (CVF) spectrometers use a rotating filter wheel to obtain one infrared spectrum every 0.5 s. The source viewed at the beginning of a scan is thus not necessarily that viewed at the end of a scan. Nevertheless, these spectrometers yield valuable data, as described below.

The ultraviolet photometers consisted of 10×10 arrays of detectors with four-position filter wheels that indexed every 0.6 s. Because the high-sensitivity photometer (HSP) developed problems in its filter wheel advancing mechanism just prior to launch, the wheel was locked with a single filter in place.

Even though the sensor module gyroscope reference was lost early in the flight, it was possible to construct a trial attitude data set based on the gyroscope raw voltages and an assumed set of references.[6] Examination of the uv data on star sightings has shown that the final attitude data used has

Received July 25, 1983; revision received Sept. 17, 1984.

*Senior Research Scientist.

†Principal Research Scientist (currently with Spectral Sciences, Inc., Burlington, Mass.).

‡Research Physicist (Optics).

§Supervisory Research Chemist.

¶MSMP Program Manager.

Table 1 Partial list of TEM-1 instruments, bandpasses, and fields of view

Instrument	Wavelength, μm	Field of view, deg
Full-field radiometer		
Channel 1	~4.3[a]	4.0×4.0
Channel 2	~2.8[a]	4.0×4.0
CVF spectrometer 1	2.15-5.44	4.0×4.0
CVF spectrometer 2	7.0-22.5	4.0×4.0
High-sensitivity photometer[b]	0.143-0.187	4.0×4.0
(each pixel)		0.4×0.4
Medium-sensitivity photometer-32[b]		4.0×4.0
Each pixel		0.4×4.0
Filter 1	~0.210	
Filter 2	~0.235	
Filter 3	~0.260	
Filter 4	~0.280	
Televison camera	Visible	21×28

[a]Actual bandpass is classified. [b]10×10 array of detectors.

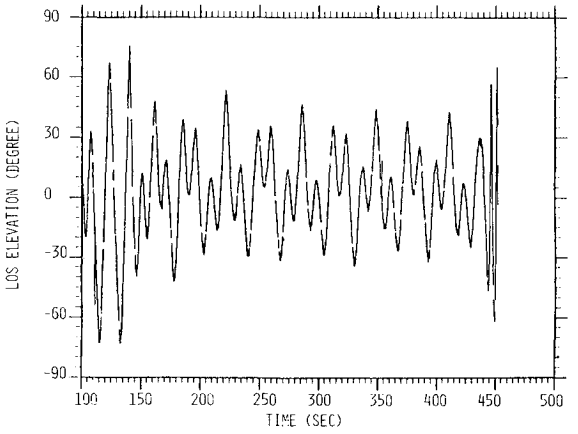

Fig. 1 Line of sight elevation angle vs time for the MSMP TEM-1 flight.

a residual error of ~ ±10 deg (2σ) both in elevation and azimuth. The final reconstruction is shown in Figs. 1 and 2.

The Aries booster is a Minuteman I second stage motor refitted to stand alone as a sounding rocket.[1] Some of its properties are listed in Table 2. Its fuel load is primarily NH_4ClO_4 and aluminum powder held together by a polyether urethane rubber binder material.[7] The case of the rocket is insulated by a layer of butadiene acrylonitrile copolymer rubber, which is loaded with asbestos or silica to prevent "cook off" following burnout of the rocket motor. The motor is considered to be "sliverless," i.e., its propellant burns out abruptly, facilitating rocket trajectory prediction. It is recognized, however, that momentary quenching and reignition of the fuel at high altitudes can occur (this is known as "chuffing"). Two possible sources for hot gas emissions from the spent booster are thus reignition of unburned fuel at high altitudes and outgassing of the rubber insulation.

Television Data

The booster was viewed by the television camera 12 times during the flight. The apparent size and shape of the images vary considerably, as shown in Fig. 3. Early in the flight, the booster appears far below the airglow layer. Soon after, it rises just above it. This suggests that the "spent" booster has

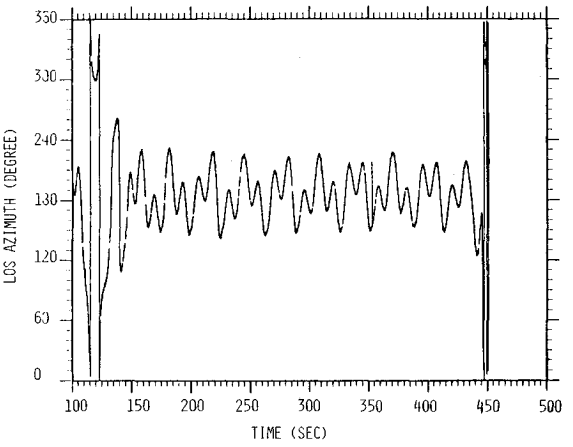

Fig. 2 Line of sight azimuth vs time for the MSMP TEM-1 flight.

some residual thrust. Table 3 gives the apparent size of the TV image of the booster and its position relative to the sensor as derived from the TV data and the attitude reconstruction.

Only the nozzles of the booster were expected to be hot enough to be visible in the TV. Thus, the TV image reflects a large contribution from "blooming" of a very bright source. The size of the TV image generally decreases with time, but it has small quasiperiodic variations. The overall decrease is expected for a source that is gradually cooling or receding, while the oscillations might be due to aspect changes if the booster is somehow tumbling as a result of payload separation or residual thrust.

Full-Field Radiometer Data

Representative FFR data are shown in Figs. 4-7. The measured background signals 150-200 s into the flight in both the 4.3 and 2.7 μm spectral regions are as much as two orders of magnitude greater than later (310-325 s) in the flight. They are thus not a result of instrument noise, which would be consistent throughout the flight.

Figures 8-11 show elevation vs azimuth plots for the background periods shown in Figs. 4-7, respectively. Comparing Figs. 4 and 8, it can be seen that high backgrounds occur for elevation angles from −10 to 45 deg and for azimuths of 150-220 deg. Figures 5 and 9 show a similar situation at a later time. Since the television data place the booster at elevation ~ −10 deg and azimuth ~180 deg, it is necessary to explore the reason why the backgrounds occur over such a large spatial range.

The simplest and most plausible explanation depends on consideration of the atmospheric mean free path (mfp). At 160 s after launch, the vehicle altitude reaches 180 km, where the mfp is >100 m. Since the booster separated from the payload at about 1 $m \cdot s^{-1}$, it is less than 1 mfp away from the sensor. The sensor, then, is apparently immersed in the cloud of hot gas that surrounds the booster and is expected to see high backgrounds in all directions. Weak maxima do occur near $t = 167$ and 190 s when the line of sight is nearest the location of the booster. This is not surprising, as the booster gases would be hotter and denser close to the booster. The shortwave infrared (SWIR) CVF data presented below indicate that the maxima are not due to the partial off-axis rejection of the Earth's radiation, since the spectra obtained at these times are dominated by molecular emission.

The data in Fig. 6 show a different situation, where the radiation source is much more narrowly defined near azimuth 175 deg, but the signals are nearly as strong at an elevation angle of 20 deg ($t = 377$ and 386 s) as they are at an elevation angle of 5 deg ($t = 380$ s). This suggests a streak or trail following the booster in its descent. At these late times, the booster is no longer visible in the television. It is reasonable to suppose

Table 2 Aries booster properties[a]

Propellant constituent		Polyurethane, 18% Ammonium perchlorate, 65% Aluminum powder, 17%	
Physical properties			
Thrust		47,000 lb	
Flow rate		173 lb/s	
No. of nozzles		4	
Expansion ratio		18	
Throat diameter		4.249 in.	
Chamber properties			
Pressure		449 psia	
Temperature		3310 K	
Exit plane properties			
Pressure		0.1983 atm	
Temperature		1575 K	
Molecular weight		26.451	
Mach No.		3.502	
Velocity		2.713 km/s	
Exit plane mole fractions (major species)			
H_2O	0.129	HCl	0.143
CO_2	0.017	Al_2O_3(s)	0.082
CO	0.236		
H_2	0.310		
N_2	0.076		

[a]From Ref. 7

Table 3 Apparent booster size and relative position from TV data

Time, s	Mean diameter[a] deg	Position elevation, deg	Position azimuth, deg
146.7	2.8	-33	176
154.5	1.8	-30.6	182.7
167.7	0.8	-15	178.7
175.7	0.6	-18.6	164
190.4	0.7	-8.5	180
202.4	1.3	-16.6	172.8
212.7	0.6	-11	172
238.0	0.0	—	—
276.0	0.2	-12.4	174.5
292.2	0.0	—	—
301.6	0.2	-9.0	171.8
317.7	0.4	-8.2	178.2
340.0	0.0	—	—
355.4	1.1	-7.0	175
364.5	0.5	-11.1	170.8
380.9	0.0	—	—
417.0	0.0	—	—
424.8	0.0	—	—
428,3	0.0	—	—

[a]An apparent size of 0.0 indicates a time when α Eridanus is in the TV field of view and the booster is expected to appear, but does not.

that by this time the nozzles have cooled enough to be dark. Hot gases may still be emitted by the combustion chamber, although surely not as much nor as hot as earlier in the flight. At $t = 364$ s, the vehicle altitude is below 155 km, where the atmospheric mfp is ~65 m.[8] The sensor is probably not immersed in a gas cloud, as it was earlier, so the background should be more confined spatially.

Three sources of the observed FFR radiation suggest themselves. It is likely that all are involved. The first is thermal emission from molecules such as CO_2 and H_2O that are formed in the Aries combustion chamber and leave it in a thermally populated excited state. The second is chemiluminescence of molecules formed in excited vibrational states of the ground electronic state by the reaction of atmospheric molecular oxygen with unburned fuel fragments. This sort of mechanism has been examined previously and observed ex-

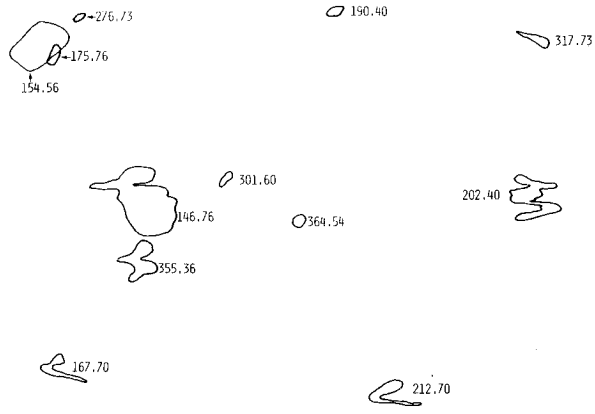

Fig. 3 Apparent TV image of booster at the indicated mission times in seconds; distortion by the TV has occurred in six cases (corners of the TV image are indicated.

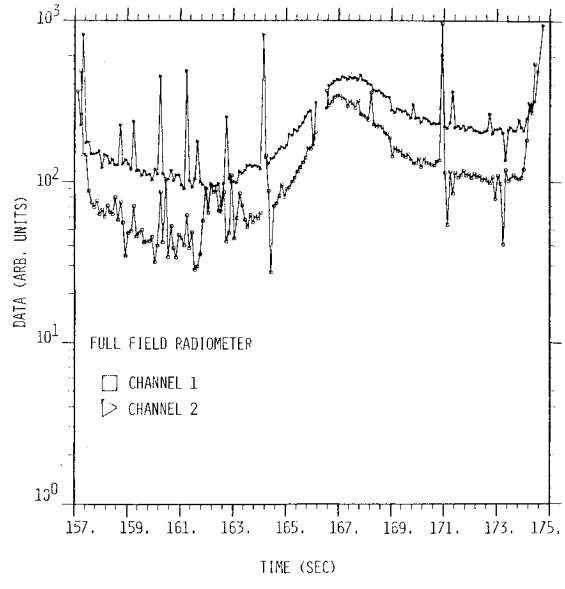

Fig. 4 TEM-1 full-field radiometer data, 157-175 s.

perimentally.[9] The third mechanism involves cascading transitions within the vibrational manifold of the ground electronic state after emission of a uv photon by an electronically excited molecule or fragment. Some uv chemiluminescent reactions possibly involved in such a mechanism will be discussed later in this report. The second and third mechanisms deserve particular attention below 165 km altitude, where the number density of O atoms increases rapidly.

Additional evidence for the O atom mechanism can be found in the data of Figs. 7 and 11. At $t = 412$ s, there is a source detected at elevation angles near 40 deg and aximuths of 155-180 deg. This signal is four times more intense than that previously recorded at nearly the same relative position. The O atom hypothesis is supported by these data, because at $t = 412$ s the altitude is 124 km and the O atom number density is five to six times higher than at 165 km.[8] In addition, the trail of exhaust gases is more confined spatially. Some further supporting evidence for the O atom reaction mechanism will be given when the ultraviolet data are discussed below.

SWIR CVF Data

Figure 12 shows a typical spectrum obtained by the shortwave infrared circular variable filter (SWIR CVF) spectrometer when the FFR recorded the spent-stage emission. The spectra include peaks corresponding to HCl. This indicates

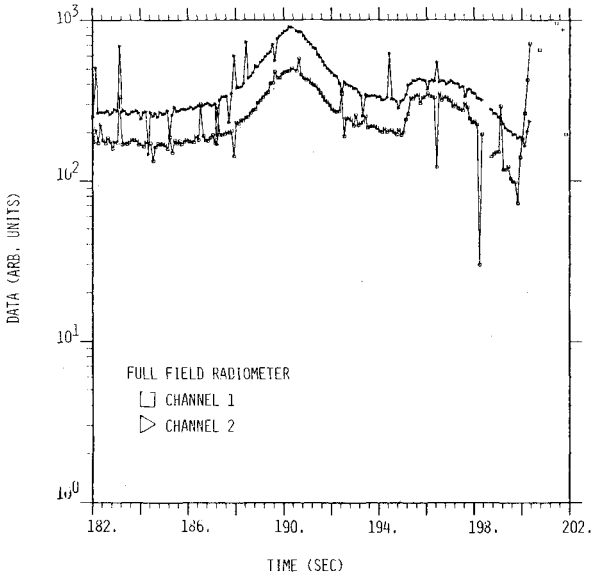

Fig. 5 TEM-1 full-field radiometer data, 182-202 s.

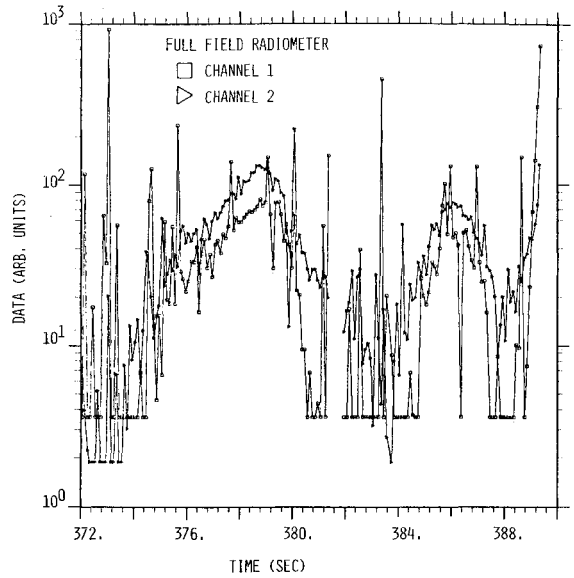

Fig. 6 TEM-1 full-field radiometer data, 372-390 s.

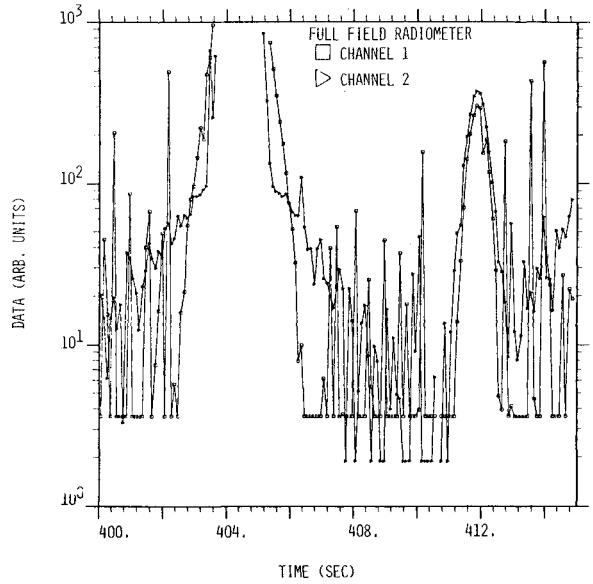

Fig. 7 TEM-1 full-field radiometer data, 400-415 s.

that the background signals are coming from the booster, since the target engine oxidizer/fuel mixture did not contain chlorine. This is consistent with the data of Table 2, which show that HCl, H_2O, and CO are the most abundant exit plane species having i.r. emissions.

Rotational Temperatures

The HCl and CO are surely vibrationally excited; but, because of the expansion into vacuum, the rotational temperature could be quite different. An estimate of the rotational temperature can be made by constructing synthetic spectra of the two species using known molecular constants and standard formulas.[10] By convoluting the source emission at an assumed rotational temperature with the instrument spectral resolution function, an expected spectrum can be constructed and compared to the data.

The results for HCl are shown in Fig. 13. The HCl spectrum is fitted best in width and R/P branch relative strength by rotational temperature between 200 and 300 K. This is low compared to an expected booster chamber temperature above 1000 K, produced by the postboost combustion of unburned propellant and indicates that the gas has undergone a mild dynamic expansion. It has also not been thermalized by the atmosphere, whose temperature is over 600 K at altitudes above 150 km.[8]

Figure 14 displays spectral data on CO along with spectra calculated using an assumed rotational temperature and the instrumental spectral resolution function. As in the case of HCl, rotational temperatures between 200 and 300 K are indicated. The similarity of the rotational temperatures of HCl and CO is consistent with their having the same source, namely combustion gases resulting from postboost chuffing having undergone a mild expansion through the booster nozzle.

By integrating each spectrum over the 3.1-3.6 μm interval and plotting the average at the corresponding time, a comparison of the HCl emission and the FFR data can be made. The integration results in peaks in the HCl emission near $t = 168$, 190, and 197 s, which is in essential agreement with the FFR data. During the period of low FFR background, $t = 310$-325 s, essentially no HCl spectral data were obtained, while some HCl spectral data were obtained from $t = 372$-390 s and weak peaks were obtained at about $t = 379$, 385, and 412 s, all in good agreement with FFR data. This further corroborates the interpretation that the FFR signals derived from the booster.

LWIR CVF Data

A typical long-wave infrared (LWIR) CVF spectrum is shown in Fig. 15 for $t = 377.3$ s, a time when the FFR and SWIR CVF show large background signals. These spectra are qualitatively different from the SWIR CVF spectra in that the signal does not go below its calibration limit between the molecular bands.

In all of the LWIR spectra, the same pattern of peaks can be found. The first, at 7.5 μm, must be viewed with some suspicion because the instrument calibration is not smooth there. Besides the CO_2 emission at 15 μm, the five other peaks are at 8.0, 8.6, 9.2, 9.8, and 12.3 μm. No known aluminum oxide species could match the observed peaks.

Since a good deal of the booster propellant and insulator were rubber, these components were investigated. Spectra of the polyether urethane rubber in the propellant were not readily available, but a spectrum of the urethane monomer was

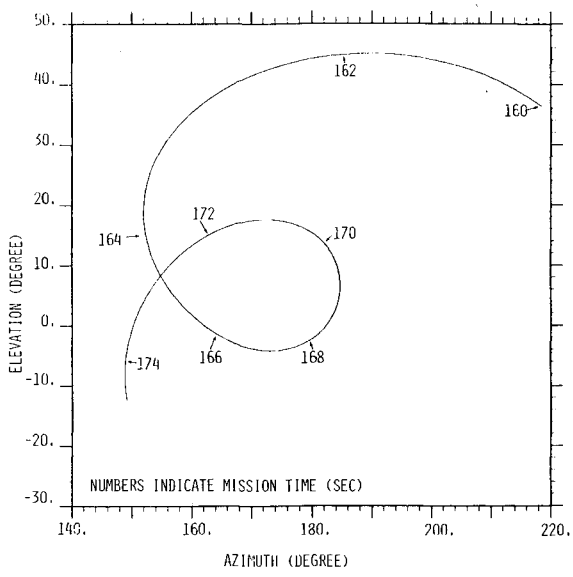

Fig. 8 TEM-1 elevation vs azimuth, 160-174 s.

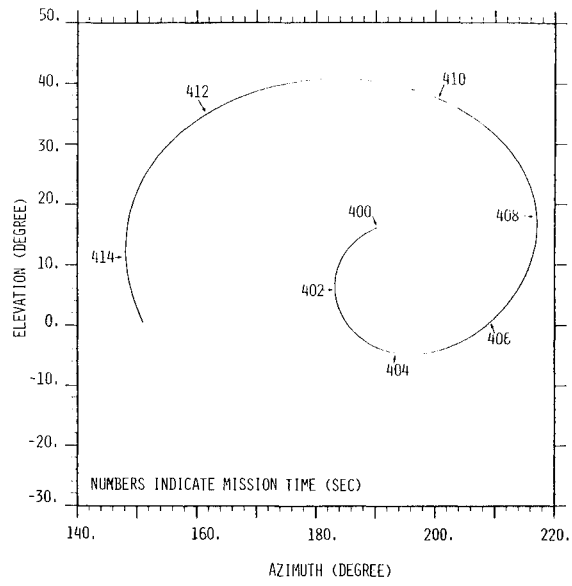

Fig. 11 TEM-1 elevation vs azimuth, 400-414 s.

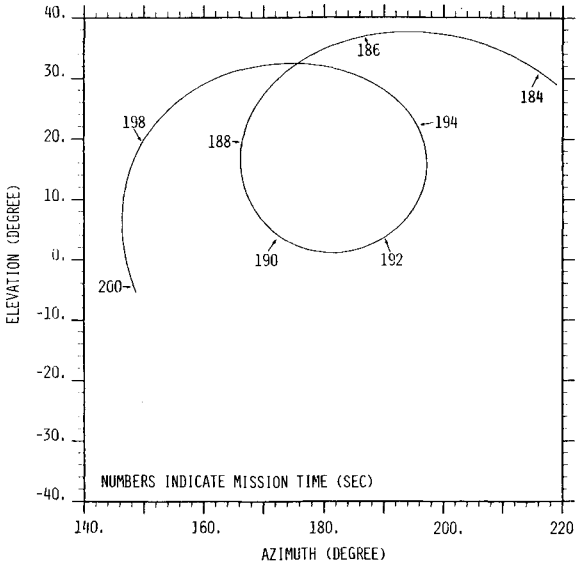

Fig. 9 TEM-1 elevation vs azimuth, 184-200 s.

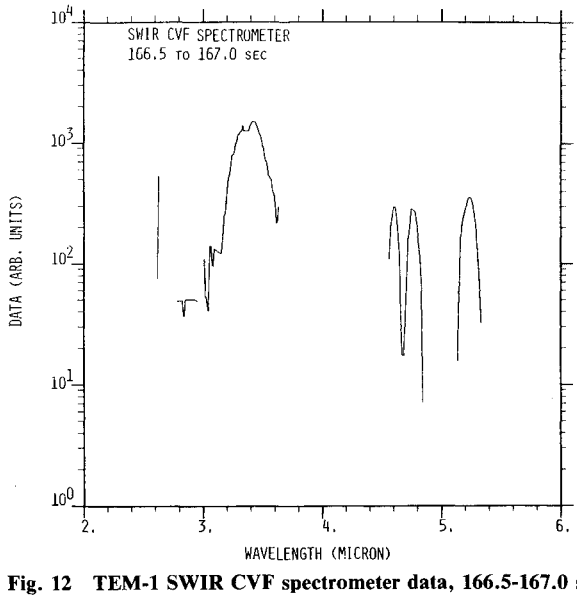

Fig. 12 TEM-1 SWIR CVF spectrometer data, 166.5-167.0 s.

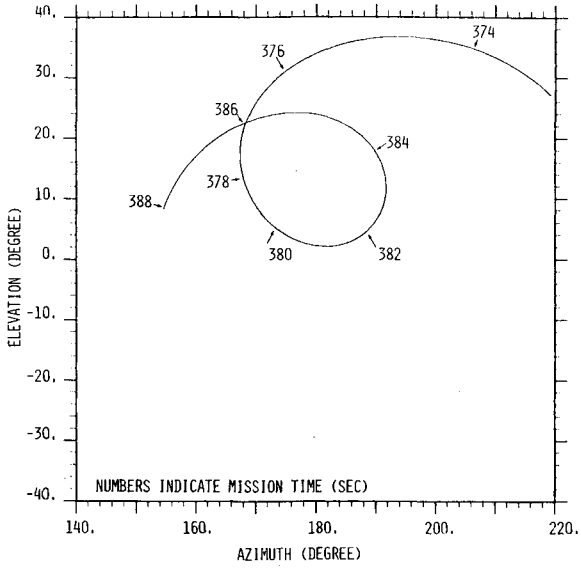

Fig. 10 TEM-1 elevation vs azimuth, 374-388 s.

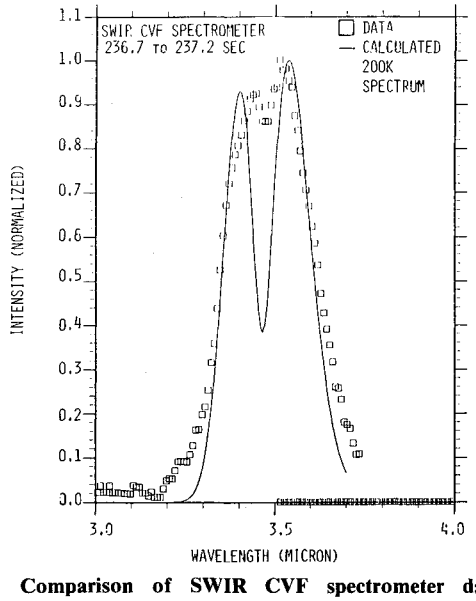

Fig. 13 Comparison of SWIR CVF spectrometer data with calculated HCl spectrum, $t = 236.7$-237.2 s.

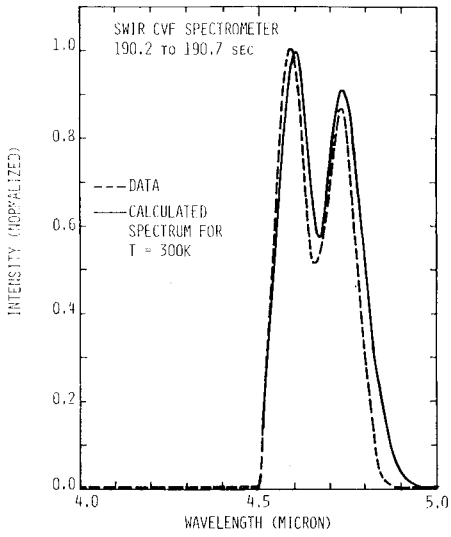

Fig. 14 Comparison of SWIR CVF spectrometer data with calculated CO spectrum, $t = 190.2$-190.7 s.

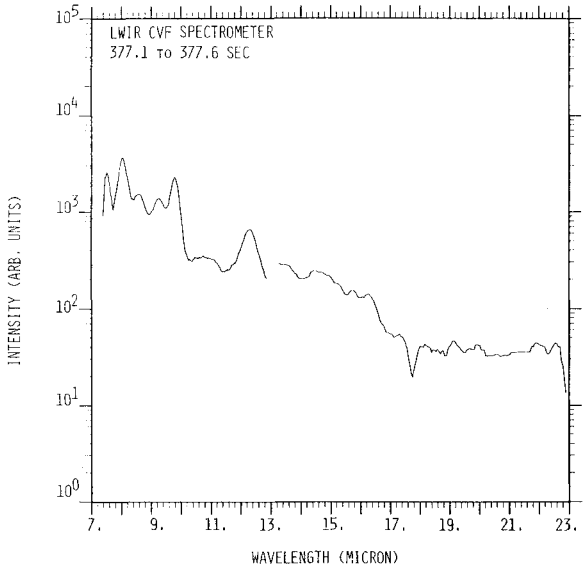

Fig. 15 TEM-1 LWIR CVF spectrometer data, $t = 377.1$-377.6 s.

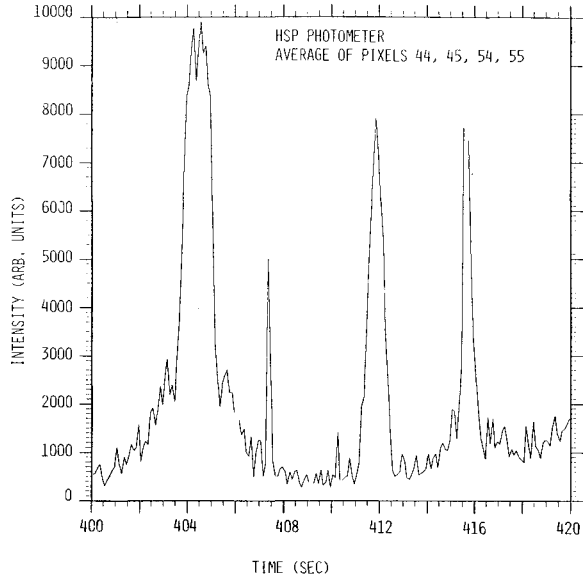

Fig. 16 TEM-1 uv high-sensitivity photometer (HSP) data, $t = 400$-420 s, average of 4 central pixels.

easily found.[11] The match between this and the TEM-1 data was not expected to be perfect, as at best the comparison would be between a polymer and its subunits. But the match was sufficiently good to be highly suggestive: urethane has absorption peaks at 7.5, 9.4, and 12.7 μm, with shoulders at 8.5, 8.7, and 9.1 μm, in generally good agreement with the LWIR CVF spectral data. The differences in the peak position and relative intensity are not outside the range of variation expected for the differences in chain length or substitution.[11] Therefore, it is likely that this instrument is recording emissions from hot organic molecules derived from the booster propellant rubber binder and insulator, as well as possible contributions from infrared chemiluminescence due to the reaction of the propellant polymer fragments with the atmospheric atomic oxygen.

Ultraviolet Data

A very prominent signal was obtained by the HSP at $t = 412$ s, as shown in Fig. 16. Figure 16 was obtained by averaging each 0.1 s frame of data from the four central pixels in the 10×10 array and plotting the result at the corresponding mission time. The peak at $t = 412$ s coincides with the data peak of the FFR and must be from the spent-stage emission. Consideration of the FFR infrared data has already suggested that the source of this signal could be chemiluminescent reactions of atmospheric oxygen atoms with molecules and molecular fragments from the booster. The existence of ultraviolet radiation at the same time makes this even more likely, because it is hard to imagine any source but a chemical reaction that could generate photons of such high energy. A possible reaction[9] is $C_2O + O \rightarrow 2\,CO(A)$, where CO(A) is the upper state of the CO fourth positive band system, which could be observed by the HSP. This emission is the chief vacuum ultraviolet (vuv) spectral feature from both permixed hydrocarbon/air flames and hydrocarbon/atomic oxygen diffusion flames.[12-18] In addition, similar emissions have been observed from rocket plumes in altitude regions were atomic oxygen is the dominant atmospheric species.[19] Another observation of vuv emission originally ascribed to a celestrial source[4] was probably due to the spent booster stage.[20]

The half-intensity points of the data are separated by 0.75 s and about 10 deg in angle. This suggests a narrow spatial extent for the radiation source. The chemiluminescent hypothesis requires that the spatial extent should be about 1 mfp. From the trajectory data, it is estimated that at $t = 412$ s the horizontal component of the booster/sensor separation would be 29 m (assuming that the separation has not been affected by residual thrust from the booster). That is how far away the "trail" left by the booster would be from the sensor, since the two are falling nearly vertically. The angular width of 10 deg implies a spatial width of 5.1 m. This is almost precisely the atmospheric mean free path[8] at 125 km and the sensor altitude at $t = 412$ s, so this aspect of the data is also consistent with the hypothesis.

MSP-32 also observed an increased signal during the 412 s event. The observed emission is probably due to excited products such as OH and NO formed from the chemiluminescent reactions[21] of the spent-stage exhaust and atmospheric atomic oxygen.

Conclusions

Analysis of the MSMP TEM-1 spent-stage emission data has shown that the spent Aries booster produces significant amounts of infrared and ultraviolet radiation that could interfere with intended radiation measurements. The interference can be seen in virtually every direction at 170 s after launch (107 s after burnout), when the booster and its instrument payload are separated by not much more than one atmospheric mean free path.

The data from several instruments show a consistent pattern of emission by H_2O, CO_2, HCl, and CO, all of which are expected to be found in the booster exhaust mixture. The rotational temperatures of CO and HCl were found to be between 200 and 300 K. This temperature is higher than that expected from a strong gasdynamic expansion of high-pressure gas through a nozzle and lower than the atmospheric temperature. This implies that the CO and HCl observed have not been greatly thermalized by the atmosphere, but have undergone a mild gasdynamic expansion through the booster nozzles.

Infrared emission by large polyatomic molecules from the booster have been observed in the 7.5-23 μm region. Ultraviolet emission from unidentified components has also been noted. The uv emissions probably derive from chemiluminescent reactions of combustion fragments with atmospheric atomic oxygen.

These analyses should provide guidance for planning and analysis of high-altitude infrared and ultraviolet radiation experiments using the Aries or other solid-fueled booster engines. It would be desirable to plan future experiments using the Aries booster to minimize the effect of this spent-stage emission.

References

[1] *Aviation Week and Space Technology,* Jan. 7, 1974, p. 34.

[2] Rogers, J. W., Stair, A. T. Jr., Wheeler, N. B., Wyatt, C. L., and Baker, D. J., "LWIR (7-24 μm) Measurements from the Launch of a Rocketborne Spectrometer Into an Aurora," Air Force Geophysics Laboratory, Rept. AFGL-TR-76-0274, Nov. 1976.

[3] Rogers, J. W., Stair, A. T. Jr., Wheeler, N. B., Wyatt, C. L., and Baker, D. J., "LWIR (7-24 μm) Measurements From the Launch of a Rocketborne Spectrometer Into a Quiet Atmosphere," Air Force Geophysics Laboratory, Rept. AFGL-TR-77-0113, May 1977.

[4] Anderson, R. C., Henry, R. C., Brune, W. H., Feldman, P. D., and Fastie, W. G., "Far Ultraviolet Studies. V. Rocket Observations of the Diffuse Cosmic Background," *Astrophysical Journal,* Vol. 234, Dec. 1979, pp. 415-426.

[5] Huffman, R. E., Paulsen, D. E., Larrabee, J. C., Baisley, V. C., LeBlanc, F. J., Frankel, D. S., and Gersh, M. E., "Vacuum Ultraviolet Airglow and Stellar Observations on the MSMP TEM-1 Rocket Flight," Air Force Geophysics Laboratory, Rept. AFGL-TR-80-0278, 1980.

[6] Sullivan, B., Boston College, Private communication, 1978.

[7] Chemical Propulsion Information Agency Rocket Motor Manual, CPIA/M1, SPIA/M1 Unit 265, May 1962.

[8] *U.S. Standard Atmosphere,* U.S. Government Printing Office, Washington, D.C., 1976.

[9] Moss, M. G., Hudgens, J. W., and McDonald, J. D., "Infrared Chemiluminescence Investigation of the Reactions of Methyl Radicals with Oxygen and Flourine," *Journal of Chemical Physics,* Vol. 72, March 1980, pp. 3486-3489.

[10] Herzberg, G., *Molecular Spectra and Molecular Structure, I. Spectra of Diatomic Molecules,* Van Nostrand and Reinhold Co., New York, 1950, pp. 111, 126.

[11] Pouchert, C. J. (ed), *The Aldrich Library of Infrared Spectra,* Aldrich Chemical Co., Inc., 1975, p. 399.

[12] Becker, D. H. and Bayes, K. D., "CO Emission from Acetylene-Oxygen Flames," *Journal of Chemical Physics,* Vol. 45, July 1966, pp. 396-397.

[13] Becker, K. H. and Bayes, K. D., "CO Chemiluminescence From Flames," *Journal of Chemical Physics,* Vol. 48, Jan. 1968, pp. 653-661.

[14] Bayes, K. D., "Spectroscopic Study of the Chemiluminescent Reaction O + CCO," *Journal of Chemical Physics,* Vol. 52, Feb. 1970, pp. 1093-1097.

[15] Shackleford, W. L., Mastrup, F. M., and Kreye, W. C., "Excitation and Quenching of CO Fourth Positive Chemiluminescence Due to Reactions Involving C_2O," *Journal of Chemical Physics,* Vol. 57, Nov. 1972, pp. 3933-3944.

[16] Kummler, R. H., Fisher, E. R., and Boyton, F. P., "Hydrocarbon Chemistry and Chemiluminescence in High Altitude Plumes," Air Force Cambridge Research Laboratory, Rept. AFCRL-TR-73-0727, Aug. 1973.

[17] Krieger, B., Malki, M., and Kummler, R., "Chemiluminescent Reactions of Oxygen Atoms with Reactive Hydrocarbons, I: 7000-9000 Å," *Environmental Science and Technology,* Vol. 6, Aug. 1972, pp. 742-744.

[18] Fontijn, A. and Johnsen, S. E., "Mechanism of CO Fourth Positive VUV Chemiluminescence in the Atomic Oxygen Reaction with Acetylene: Production of $C(^3P,^1D)^*$," *Journal of Chemical Physics,* Vol. 59, Dec. 1973, pp. 6193-6200.

[19] Draper, J. S., Bien, F., Huffman, R. E., and Paulsen, D. E., "Rocket Plumes in the Thermosphere," *AIAA Journal,* Vol. 13, June 1975, pp. 825-827.

[20] Price, S. D., Murdock, T. L., McIntyre, A., Huffman, R. E., and Paulsen, D. E., "On the Diffuse Cosmic Ultraviolet Background from Aries A-8," *Astrophysical Journal,* Vol. 240, Aug. 1980, pp. L1-L2.

[21] Gaydon, A. G., *The Spectroscopy of Flames,* John Wiley & Sons, New York, pp. 195 and 252.